Symmetry-resolved K-shell photoabsorption spectra of free N_2 molecules

E. Shigemasa, K. Ueda,* Y. Sato,* T. Sasaki, and A. Yagishita
Photon Factory, National Laboratory for High Energy Physics, Oho 1-1, Tsukuba-shi, Ibaraki-ken 305, Japan
(Received 11 October 1991)

"Symmetry-resolved" photoabsorption spectra of free N_2 molecules in the K-shell excitation region have been obtained using a technique of angle-resolved photoion spectroscopy combined with linearly polarized undulator radiation. The obtained Σ- and Π-symmetry component spectra have nicely demonstrated the symmetry decomposition of the photoabsorption spectrum. These spectra have been compared with theoretical calculations in the photon-energy regions below and above the ionization threshold.

PACS number(s): 33.80.Eh, 33.80.Gj

I. INTRODUCTION

A. Historical review

Since Nakamura *et al.* [1] revealed the Rydberg states in the K-shell photoabsorption spectrum of nitrogen molecules in 1969, much experimental and theoretical work has been performed on the K-shell photoabsorption of molecules [2]. General features of the K-shell photoabsorption spectra of first-row diatomic molecules have been made clear by those intensive investigations [1,3–10]. The structures in the spectra have been assigned to a strong transition of a K-shell electron to an unoccupied valence orbital with π symmetry, weak transitions to Rydberg orbitals with σ or π symmetry, and transitions enhanced by a shape resonance to continuum orbitals with σ symmetry.

The molecular photoabsorption is highly anisotropic because the excited states have definite symmetries as mentioned above. As a consequence of the dipole selection rules, the excitation of π resonances yields molecules preferentially excited perpendicular to the electric vector of the incident light, while the excitation of σ resonances produces molecules selectively excited parallel to the electric vector. In 1980, Dill *et al.* [11] developed a theory describing the molecular orientations of K-shell-excited molecules which have definite symmetries. In their paper the authors pointed out that the angular distribution of the emitted Auger electrons would be related to the molecular orientations, because the subsequent decay of the K-shell vacancy is a fast process compared with molecular rotation. Along this theoretical prediction, several experiments on the anisotropic Auger-electron emission have been performed [12–14]. In contrast to the theoretical prediction, Truesdale *et al.* [12] observed that the Auger-electron emission from K-shell-excited CO showed nearly isotropic decay behavior. Lindle *et al.* [13] observed the similar isotropic decay behavior for K-shell-excited N_2. The more sophisticated work by Becker *et al.* [14] showed that the Auger-electron emission at the strong resonance into the π^* orbital followed the theoretically predicted behavior in contrast to the former experimental work, whereas the Auger electron was emitted isotropically at the σ shape resonance, unaffected by the anisotropic photoexcitation process.

To resolve the puzzling disagreement between the experimental results and the theoretical prediction, we have applied angle-resolved photoion spectroscopy to determine the molecular orientations of K-shell-excited molecules [15,16]. Fragment-ion measurements, which have been performed not only by us [15,16] but also by other authors [17,18], have resolved the puzzling disagreement. Prominent anisotropic angular distributions of the fragment ions, depending on the photon energies, have been observed in these experiments. Continuing our previous work [15,16], we report in this paper the "symmetry-resolved" K-shell photoabsorption spectra of N_2. This spectroscopy permits the symmetry decomposition of the continuum states as well as the identification of the symmetry of discrete excited states.

B. Theoretical background

The molecular orientation will directly be reflected in the angular distribution of fragment photoions, because the fragment photoions are immediately emitted from a repulsive potential of the molecular ions, which is caused by a subsequent Auger decay of the K-shell vacancy (the axial-recoil approximation [19] may be applied). Since the angular distribution of the photoions is more intuitive to represent the anisotropic photoabsorption, we refer hereafter to the angular distribution of the photoions instead of the molecular orientation. We use total symmetries for representing the symmetries of the ground and excited states.

For randomly oriented molecules with cylindrical symmetry in the gas phase, within the framework of the dipole approximation, the expression for the angular distribution $d\sigma/d\Omega$ of photoions produced by the excitation with linearly polarized light may be written in the form [20,21]

$$\frac{d\sigma}{d\Omega}=\frac{\sigma}{4\pi}\left[1+\frac{\beta}{2}(3\cos^2\theta-1)\right], \tag{1}$$

where θ is the angle between the electric vector of the in-

cident light and the emitted photoion directions, and β is the asymmetry parameter characterizing the angular distribution of the photoions. The asymmetry parameter is defined as the difference between the photoabsorption strengths D_Λ^2 for molecular orientation parallel to (Σ) or perpendicular to (Π) the electric vector of the light:

$$\beta=\frac{2(D_\Sigma^2-D_\Pi^2)}{D_\Sigma^2+2D_\Pi^2} . \tag{2}$$

Because the photoabsorption cross section σ is the sum of the photoabsorption strengths, i.e., $\sigma=4\pi^2\alpha h\nu(D_\Sigma^2+2D_\Pi^2)/3$ (α is the fine-structure constant and $h\nu$ is the photon energy), the differential cross section for the direction parallel to the electric vector gives the Σ-symmetry component of the photoabsorption cross section [as derived from Eqs. (1) and (2)]:

$$\left.\frac{d\sigma}{d\Omega}\right|_{\theta=0^\circ}=\frac{3}{4\pi}\sigma_\Sigma , \tag{3}$$

and the differential cross section for the direction perpendicular to the polarization vector gives the Π-symmetry component of the photoabsorption cross section:

$$\left.\frac{d\sigma}{d\Omega}\right|_{\theta=90^\circ}=\frac{3}{4\pi}\frac{\sigma_\Pi}{2} . \tag{4}$$

Here we have introduced the symbols

$$\sigma_\Sigma=4\pi^2\alpha h\nu D_\Sigma^2/3 \tag{5}$$

and

$$\sigma_\Pi=4\pi^2\alpha h\nu 2D_\Pi^2/3 \tag{6}$$

for the $\Sigma\rightarrow\Sigma$ and $\Sigma\rightarrow\Pi$ symmetry-resolved photoabsorption cross sections.

As shown in Eqs. (3) and (4), $d\sigma/d\Omega|_{\theta=0^\circ}$ measured as a function of photon energy forms the Σ-symmetry component spectrum of the K-shell photoabsorption, and $d\sigma/d\Omega|_{\theta=90^\circ}$ forms the Π-symmetry component spectrum. It should be noted that $d\sigma/d\Omega|_{\theta=0^\circ}$ is proportional to σ_Σ, while $d\sigma/d\Omega|_{\Theta=90^\circ}$ is proportional to $\sigma_\Pi/2$.

II. EXPERIMENT

A. Experimental setup

The experiments have been performed on beam line BL-2B supplying the synchrotron radiation emitted from an undulator [22] inserted in the 2.5-GeV storage ring at the Photon Factory. The radiation is monochromatized by a 10-m grazing-incidence monochromator [23] equipped with a Au-coated replica grating of 1200 grooves/mm. This monochromator can provide soft x rays ranging from 260 to 1800 eV. The entrance- and exit-slit widths were set to 50 μm. The corresponding bandpass was about 0.6 eV at $h\nu=400$ eV and the photon flux was approximately 10^{12} photons/sec at the maximum.

The experimental setup is shown schematically in Fig. 1. The monochromatized photon beam was focused

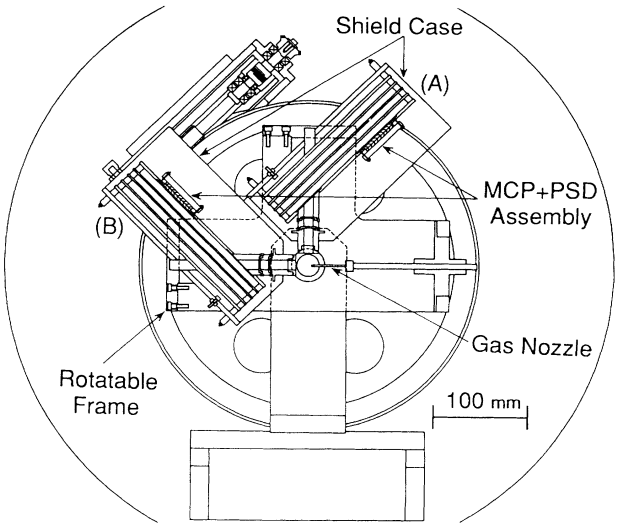

FIG. 1. Schematic drawing of the experimental apparatus. Two identical parallel-plate electrostatic analyzers labeled (A) and (B) are positioned at 90° and 0°, respectively, relative to the electric vector of the incident light (MCP means microchannel plate and PSD means position-sensitive detector).

onto the center of the interaction region. The cross section of the photon beam in this region was less than 1×1 mm^2. The sample gas was injected into the region through a nozzle with a diameter of 0.8 mm. The background pressure in the chamber was 1×10^{-5} Torr when the sample gas was introduced. The photoions emerging from the interaction region were energy analyzed by two identical parallel-plate electrostatic analyzers [24] with position-sensitive detectors. The analyzers were positioned to detect the photoions emitted at 0° and 90° relative to the electric vector of the incident light. The effective acceptance angle of the analyzers was estimated to be about ±2°. The whole kinetic-energy spectra for the photoions from N_2 can be measured with a given deflection voltage of the analyzers. The spectra are composed of two major peaks [11]; a peak near zero kinetic energy corresponds to molecular ions with thermal energy, and a broad peak centered at around 5 eV is attributed to fragment ions. In order to detect only the broad peak (>2 eV) from the whole spectrum, an appropriate deflection voltage was applied to each analyzer. Under this condition, the spectra σ_Σ and $\sigma_\Pi/2$ were obtained simultaneously by counting the signals from each detector as a function of the photon energy. The photon intensity was monitored with a gold mesh after the exit slit of the monochromator to normalize the spectra. The photon-energy scale was calibrated on the basis of the electron energy-loss spectra reported by Hitchcock and Brion [9].

The different detection efficiencies of the two analyzers have been corrected as follows. N 1s photoelectrons from N_2 have been measured with the analyzers positioned at 0° and 90° relative to the electric vector and asymmetry parameters have been derived from their intensities. Our asymmetry parameters differ from those of Lindle *et al.*

[13] because of the different detection efficiencies. The correction coefficient for the detection efficiencies has been determined to give the same values as the asymmetry parameters of Lindle *et al.* [13].

The spectra σ_Σ and $\sigma_\Pi/2$ are composed of the valence and K-shell contributions. The valence contributions are considered as being constant in the K-shell excitation region. We have subtracted the constant valence contributions from the spectra. These subtractions have been done for spectra displayed in the following sections.

B. Evaluation of the degree of polarization

The degree of linear polarization of the undulator radiation with a limited divergence angle of 0.066 mrad had previously been determined by measuring the angular distribution of photoelectrons from helium, and turned out to be 100% at the top of the first harmonic [25]. Although the undulator radiation is reflected horizontally by six optical elements within the beam line [23], it can be assumed that the monochromatized radiation is 100% linearly polarized at the top due to the inherent polarization of the primary undulator radiation.

In the present work, the peak of the first harmonic was fixed at a photon energy of 435 eV when the K-shell photoabsorption spectra of N_2 were measured. The undulator-radiation spectrum monitored with drain current from a gold mesh is shown in Fig. 2. The degree of linear polarization within the first harmonic slightly depends on the photon energy. At the top, the degree of polarization reaches the maximum as mentioned above. According to the calculation by Kitamura [26], the polarization of the primary undulator radiation ranges from 95% to 100% in the whole energy region displayed in Fig. 2.

If the asymmetry parameter β for the photoions is known, which is the case for the π^* resonance of N_2 at 401.0 eV, one can determine the degree of polarization from the angular distribution of the photoions. We have estimated the polarization of the incident light from the differential cross sections $d\sigma/d\Omega|_{\theta=0^\circ}$ and $d\sigma/d\Omega|_{\theta=90^\circ}$ for the π^* resonance. As a result, it turned out that the degree of linear polarization at 401.0 eV, lying at the lower-energy tail in the spectrum of the first harmonic shown in Fig. 2, was 95%. This is consistent with the calculation by Kitamura [26]. Obviously, the high degree of linear polarization is of great advantage in the studies for symmetry-resolved photoabsorption spectra.

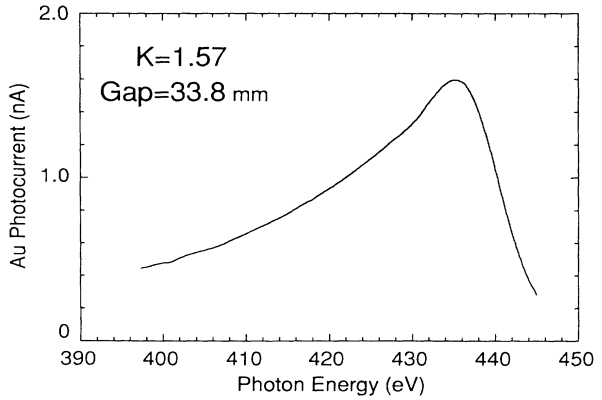

FIG. 2. Undulator-radiation spectrum at beam line BL-2B of the Photon Factory. The intensity was monitored with drain current from a gold mesh after the exit slit of the monochromator. The peak position of this first harmonic was fixed at a photon energy of 435 eV during the measurements.

III. RESULTS AND DISCUSSIONS

A. Overview

Figure 3(a) shows a K-shell photoabsorption spectrum of N_2 and $(\sigma_\Sigma+\sigma_\Pi)$. The solid line represents the photoabsorption spectrum and the dots represent the sum of the σ_Σ and σ_Π symmetry-resolved spectra. Figure 3(b) shows the σ_Σ and σ_Π symmetry-resolved photoabsorption spectra which are represented by the dots and solid line, respectively. The spectra of Fig. 3(a) have been normalized relative to each other at 445 eV. In order to ob-

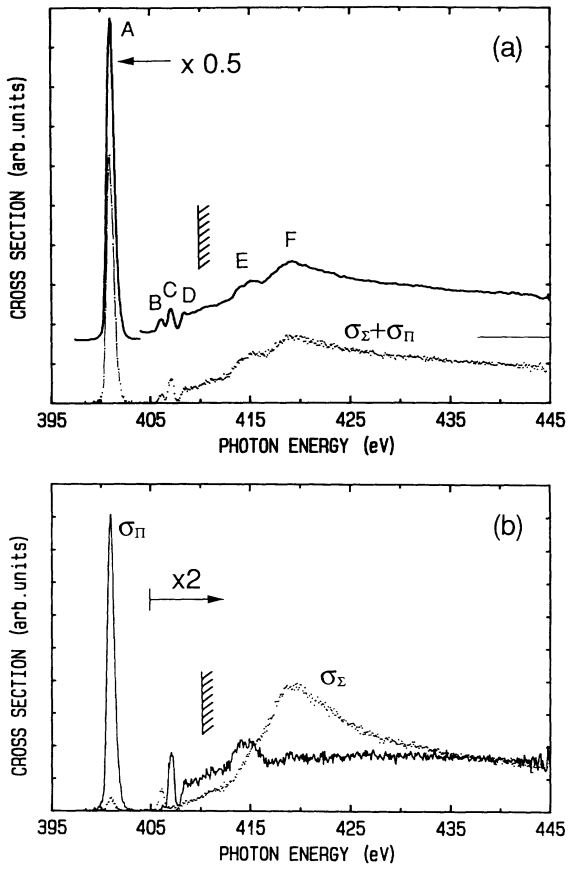

FIG. 3. (a) K-shell photoabsorption spectrum of N_2 (solid line) and sum spectrum (dots) of σ_Σ and σ_Π symmetry-resolved photoabsorption spectra $(\sigma_\Sigma+\sigma_\Pi)$ and (b) σ_Σ and σ_Π symmetry-resolved photoabsorption spectra. Notice the offset used to plot the solid line. The two spectra in (a) are relatively normalized in height at 445 eV. The dots and solid line in (b) represent σ_Σ and σ_Π, respectively.

tain σ_Π, the measured $d\sigma/d\Omega|_{\theta=90°}$ has been multiplied by a factor of 2 [see Eq. (4)]. σ_Σ and σ_Π nicely demonstrate the symmetry decomposition of the photoabsorption spectrum.

The K-shell photoabsorption spectrum in Fig. 3(a) was obtained by counting total ions with a channeltron placed at the distance of 15 mm from the ionization region. A voltage of -2.5 kV was applied to the entrance of the channeltron to detect the total ions. The spectral features (A–F) of the present photoabsorption spectrum are very similar to those observed in the photoabsorption [8] and electron energy-loss spectra [3,9]. However, quantitative comparison between the present photoabsorption spectrum and the electron energy-loss spectrum of Hitchcock and Brion [9] reveals that the intensity ratio of the present spectrum to the energy-loss spectrum [9] is about 0.7 at the π^* resonance (A) when the two spectra are normalized at the σ^* shape resonance (F) in the continuum region. This implies that the ratio of the detection efficiency of the ionization events at the π^* resonance to those at the σ^* shape resonance is about 0.7 in the present total-ion measurement. This is attributable to the difference in the ion-yield efficiency between the two resonances below and above the K-shell ionization threshold.

Comparing the two spectra in Fig. 3(a), the overall spectral profile of $(\sigma_\Sigma+\sigma_\Pi)$ is quite similar to the absorption spectrum except for the intensity at peak A. The intensity ratio of $(\sigma_\Sigma+\sigma_\Pi)$ to the absorption spectrum is about 0.4 at the π^* resonance. Therefore the intensity ratio of $(\sigma_\Sigma+\sigma_\Pi)$ to the electron energy-loss spectrum [9] is about 0.3 at this resonance. This suggests that the branching ratios generating the energetic (>2 eV) and nonenergetic (<2 eV) fragment ions are about 0.3 and 0.7, respectively, because we detected only the energetic (>2 eV) fragment ions to obtain the σ_Σ and σ_Π spectra.

The most probable decay process of the π^* resonance is the resonant Auger transition leading to a singly charged molecular ion which may dissociate into a neutral atom and an atomic ion ($N+N^+$). The resonant Auger spectrum at the π^* resonance of N_2 has been observed and the four major peaks in the spectrum have been tentatively assigned to various electron-hole configurations [27,28]. Two types of deexcitation have been apparent in the Auger spectrum. One is the so-called participant Auger decay leading to valence one-hole states, and the other is spectator Auger decay leading to valence two-hole, one-electron states.

As discussed by Saito and Suzuki [29], the origin of the production of the nonenergetic (<2 eV) fragment ions may be attributable to the outer-valence ($2s\sigma_u$, $2p\pi_u$, $2p\sigma_g$) one-hole, and the outer-valence two-hole, one-electron states. The outer-valence one-hole states do not lead to the dissociation [30]. The undissociated N_2^+ ion with thermal energy was essentially found only at the π^* resonance, and the branching ratio of this ionic species at this resonance was about 0.1 [27]. As a result, the branching ratio generating the nonenergetic (<2 eV) fragment ions from the outer-valence two-hole, one-electron states is about 0.6 of the cross section of the π^* resonance. This is roughly equal to the ratio of the peak intensity corresponding to the outer-valence two-hole, one-electron states to the total intensity in the resonant Auger spectra [27,28].

Saito and Suzuki also suggested that the inner-valence ($2s\sigma_g$) one-hole, inner-valence–outer-valence two-hole, one-electron, and inner-valence two-hole, one-electron states should lead to the production of the energetic fragment ions [29]. The peak intensity corresponding to such hole states in the resonant Auger spectra can be estimated to be about half of that of the outer-valence two-hole, one-electron states. Thus the branching ratio generating the energetic fragment ions through the inner-valence one-hole, inner-valence–outer-valence two-hole, one-electron, and inner-valence two-hole, one-electron states is estimated to be about 0.3. This is in good agreement with the above estimation of the branching ratio. Double Auger decay leading to valence two-hole states also should contribute to the product of the energetic fragment ions. The contribution of the double Auger decay to the branching ratio of the energetic fragment-ion production is within the uncertainty of 10% for this evaluation procedure.

In the symmetry-resolved σ_Σ spectrum of Fig. 3(b), only the excited states with Σ symmetry may appear. The σ_Σ spectrum is composed of a strong broad structure due to the σ^* continuum shape resonance and weak peaks corresponding to Rydberg states with Σ symmetry. It should be mentioned that the weak peak at 401.0 eV is accounted for by a vertical polarization component from the off-peak undulator spectrum, as discussed in Sec. II B. In the symmetry-resolved σ_Π spectrum of Fig. 3(b), only the excited states with Π symmetry appear. The σ_Π spectrum is comprised of the intense peak for an excitation to the $2p\pi_g$ state, weak peaks for Rydberg states, and a rather strong structure for doubly excited states.

B. Discrete resonances

Figure 4 shows the symmetry-resolved photoabsorption spectra (σ_Σ and σ_Π) below the K-shell ionization threshold of N_2. In the σ_Π spectrum, an intense peak A

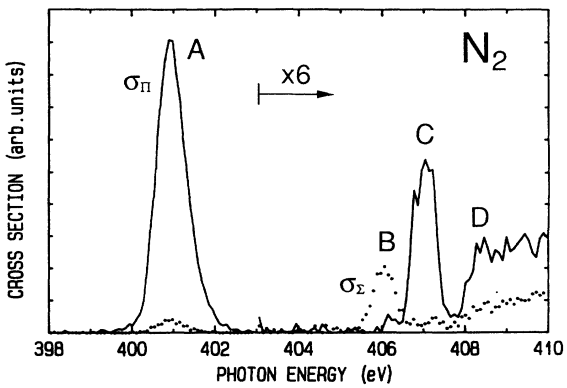

FIG. 4. Symmetry-resolved σ_Σ and σ_Π photoabsorption spectra below the K-shell threshold of N_2. The dots represent σ_Σ and the solid line represents σ_Π.

and a weak peak C are seen. Peak A corresponds to a promotion of a $1s\sigma$ electron into the $2p\pi_g$ valence orbital. Peak C corresponds to a promotion of a $1s\sigma$ electron into the $3p\pi_u$ Rydberg orbital. In the σ_Σ spectrum, the weak peak B corresponding to the promotion of a $1s\sigma$ electron into the $3s\sigma_g$ Rydberg orbital is seen. The present symmetry-resolved spectra that determine the symmetries of the excited states confirm the previous assignments [1,8–10,31–36] for these peaks.

Overlapping with peak C in the σ_Π spectrum, a very weak peak can be seen in σ_Σ. This is attributable to a $1s\sigma \rightarrow 3p\sigma_u$ transition, which has not been resolved despite high-resolution photoabsorption [36], because of both the natural width and the vibrational sideband of the main $3p\pi_u$ Rydberg state. The intensity ratio of σ_Σ to σ_Π at 407.3 eV is about 0.1.

Between 408.0 and 410.0 eV, σ_Σ and σ_Π exhibit some weak structures D which are associated with excitations to unresolved Rydberg states. Tronc, King, and Read [10] have observed the corresponding Rydberg states in their pseudophotoabsorption spectrum and assigned the structures to excitations to a $3d\pi$ Rydberg state and $np\pi$ ($n \geq 4$) Rydberg series. However, Chen, Ma, and Sette [36] assigned those as follows: based on equivalent-core model analyses, the structures revealed in their high-resolution spectrum between 408.0 and 410.0 eV have been composed of major $ns\sigma$ and minor $np\pi$ ($n \geq 4$) Rydberg series. The peak at 408.4 eV observed in their work has been tentatively assigned to the $1s\sigma \rightarrow 4s\sigma$ Rydberg transition. Although the fine structures of the Rydberg states can hardly be seen owing to our limited resolution in Fig. 4, the σ_Π spectrum is predominant between 408 and 410 eV. Thus this result supports the assignments of Tronc, King, and Read [10]. We propose here that the photoabsorption in this region is composed of the $nd\pi$ ($n \geq 3$) and $np\pi$ ($n \geq 4$) Rydberg series as the major components and the $ns\sigma$ ($n \geq 4$), $np\sigma$ ($n \geq 4$), and $nd\sigma$ ($n \geq 3$) series as the minor components.

The proposed assignments, excitation energies, and relative intensities for the spectral features shown in Fig. 4 are given in Table I with comparison to theoretical results [32,35]. The intensity of the $3p\pi_u$ was used for each normalization. The present results support the theoretical calculations by Barth and Schirmer [35] both regarding assignments and intensities.

C. Double excitation and continuum shape resonance

Figure 5 shows the symmetry-resolved σ_Σ and σ_Π photoabsorption spectra together with *ab initio* calculations above the *K*-shell ionization limit. The dashed curves represent the results of multiple-scattering $X\alpha$ calculations by Dehmer and Dill [31] with the Π component normalized to the experimental σ_Π at 445 eV. The dot-dashed curves represent results of Stieltjes-Tchebycheff moment-theory calculations by Rescigno and Langhoff [32] with the Π component normalized to the experimental σ_Π at 425 eV. Double excitations are not taken into account in these calculations.

For the Σ-symmetry component, the broad band assigned as a σ^* shape resonance spreads over the whole energy region. The peak energy position and width of the shape resonance are 419 and about 20 eV, respectively. Although the calculations give a qualitative description for the present symmetry-resolved σ_Σ, there are considerable quantitative differences. For the $X\alpha$ calculations, the peak intensity of the σ^* shape resonance is overestimated and the width is underestimated. The calculated energy position of this resonance is about 422 eV, which is about 3 eV higher than the experimental value of 419 eV. The width of the resonance is about 4 eV. For the moment-theory calculations the energy position of the resonance is around 416 eV, which is about 3 eV lower than the experimental value, and the width of the σ^* resonance is about 15 eV.

For the Π-symmetry component, the bump due to the double excitations is clearly seen around 414 eV. Neglecting the contribution of the double excitations, σ_Π increases monotonically up to 417 eV and becomes almost constant above 417 eV. The $X\alpha$ results for the Π-symmetry component give a broad maximum around 423 eV, while the moment-theory calculations give an almost constant cross section. The monotonically increasing behavior of the present σ_Π spectrum up to 417 eV is reproduced by the $X\alpha$ calculations rather than the moment-theory calculations.

In the case of the $X\alpha$ calculations, the intensity of σ_Σ relative to σ_Π differs from the present result, especially at each side of the σ^* shape resonance. σ_Σ is too small relative to σ_Π at both the photon-energy regions below 416 and above 426 eV, because the calculated bandwidth of

TABLE I. Assignments, excitation energies, and relative intensities for discrete resonances in the symmetry-resolved *K*-shell photoabsorption spectra of N_2 with a comparison to theoretical results (Refs. [32] and [35]).

Present work			Barth and Schirmer (Ref. [35])			Rescigno and Langhoff (Ref. [32])		
Assignment	Excitation energy (eV)	Relative intensity	Assignment	Excitation energy (eV)	Relative oscillator strength	Assignment	Excitation energy (eV)	Relative oscillator strength
$2p\pi_g$	401.0	10.1	$1\pi_g(\pi^*)$	400.21	27.0	$1\pi_g(\pi^*)$	396.9	17.5
$3s\sigma_g$	406.1	0.38	$4\sigma_g(3s)$	405.62	0.38	$4\sigma_g(3s)$	406.2	0.16
$3p\pi_u$	407.0	1.0[a]	$2\pi_u(3p)$	406.64	1.0[a]	$2\pi_u(3p)$	407.1	1.0[a]
$3p\sigma_u$	407.3	0.08	$3\sigma_u(3p)$	406.58	0.04	$3\sigma_u(3p)$	407.4	0.01
$3d\sigma_g$	408.0	0.02	$5\sigma_g(3d)$	407.68	0.02	$2\pi_g(3d)$	408.5	0.11
$3d\pi_g$	408.3	0.55	$2\pi_g(3d)$	407.89	0.41	$3\pi_u(4p)$	408.6	0.28

[a]The peak intensity of the $3p\pi_u$ Rydberg state was used for the normalization in each case.

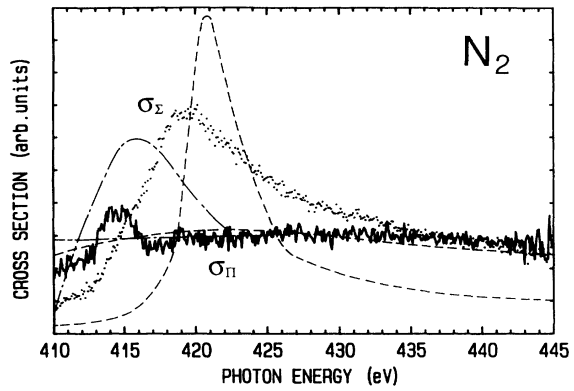

FIG. 5. Symmetry-resolved σ_Σ (dots) and σ_Π (solid line) photoabsorption spectra above the K-shell threshold of N_2. The dashed curve is the theoretical calculation by Dehmer and Dill (Ref. [31]) with the Π component normalized to the experimental σ_Π at 445 eV. The dot-dashed curve represents the theoretical calculation by Rescigno and Langhoff (Ref. [32]) with the Π component normalized to the experimental σ_Π at 425 eV.

the σ^* resonance is too narrow. The quantitative disagreement between the $X\alpha$ calculations and the present results may indicate the inaccurate representation of the R dependence of the scattering potential in the continuum multiple-scattering model. The moment-theory calculations reproduce the present partial cross sections in both the shape of the σ^* resonance and its intensity relative to the Π-symmetry cross section, although the calculated peak position of the resonance is 3 eV higher than the experimental value. However, these calculations have been performed only in the limited photon-energy region ranging from 410 to 425 eV. The quantitative discrepancies between the moment-theory calculations and the present results may be attributable to core relaxation. In the moment-theory calculations, the frozen-core Hartree-Fock approximation was used. As discussed by Lynch and McKoy [37], the use of the frozen-core approximation essentially underestimates the excitation energy and width of the σ^* resonance. Although there are many reasons the discrepancies between the experimental and theoretical results are produced, the most probable origin of these discrepancies is essentially attributable to the simplicity of a single-particle model. The $X\alpha$ and moment-theory calculations have been carried out based on the single-particle description. We hope that more sophisticated calculations including the many-electron effects are performed.

The contribution of the doubly excited states with Π symmetry could not be seen in previous reports on determinations of the molecular asymmetry parameters [15–18]. As mentioned in Sec. I B, the β parameter is represented by the intensity difference between $d\sigma/d\Omega|_{\theta=0^\circ}$ and $d\sigma/d\Omega|_{\theta=90^\circ}$ [see Eq. (2)]. Because the contribution of the σ^* shape resonance is larger than that of the double excitations around 415 eV, as seen in Fig. 4, the β values become positive. The major configurations of the doubly excited states have been assigned already [34,36]. According to the configuration-interaction (CI) calculations by Arneberg *et al.* [34], the main configurations of the doubly excited states have been interpreted as being due to the $1s\sigma \rightarrow \pi^*$ resonance transition with a $2p\pi \rightarrow 3p\pi$ shakeup transition. Chen, Ma, and Sette [36] have reported similar tentative assignments for the double excitations, which are based on analyses of the measured high-resolution photoabsorption spectrum by comparing with the optical-transition data of NO. The present result for the double excitations supports the interpretations by Arneberg *et al.* [34] and Chen, Ma, and Sette [36], that is, the total symmetry of the doubly excited states is Π.

IV. SUMMARY

We have presented an observation of symmetry-resolved K-shell photoabsorption spectra of N_2. Because it has been confirmed in this work that the degree of the linear polarization of the undulator radiation is more than 95%, the present σ_Σ and σ_Π are almost perfect symmetry decompositions of the photoabsorption spectrum. As a result, definite assignments for the symmetries of the K-shell-excited states have been given in the photon-energy regions below and above the ionization threshold. The behavior of the present σ_Σ and σ_Π in the σ^* shape-resonance region is in qualitative agreement with the theoretical calculations by Dehmer and Dill [31] and Rescigno and Langhoff [32], but there are significant quantitative discrepancies. For the double excitations, the present result supports the interpretations by Arneberg *et al.* [34] and Chen, Ma, and Sette [36].

ACKNOWLEDGMENTS

We are grateful to the staff of the Photon Factory for the stable operation of the storage ring during the course of the experiments. We would like to thank Dr. K. R. Bauchspieß for his careful reading of the manuscript. This work has been performed under approval of the Photon Factory Advisory Committee (Proposal No. 88-185).

*Permanent address: Research Institute for Scientific Measurements, Tohoku University, Katahira 2-1-1, Sendai-shi, Miyaki-ken 980, Japan.

[1] M. Nakamura, M. Sasanuma, S. Sato, M. Watanabe, H. Yamashita, Y. Iguchi, A. Ejiri, S. Nakai, S. Yamaguchi, T. Sagawa, Y. Nakai, and T. Oshio, Phys. Rev. **178**, 80 (1969).

[2] For example, *EXAFS and Near Edge Structure,* edited by A. Bianconi, L. Incoccia, and S. Stipcich, Springer Series in Chemical Physics Vol. 27 (Springer-Verlag, New York, 1983); I. Nenner, *Electron and Atomic Collisions,* edited by H. B. Gilbody, W. R. Newell, F. H. Read, and A. C. H.

Smith (North-Holland, Amsterdam, 1988), p. 517, and references therein.
[3] G. R. Wight, C. E. Brion, and M. J. Van der Wiel, J. Electron Spectrosc. Relat. Phenom. **1**, 457 (1972/1973).
[4] G. R. Wight and C. E. Brion, J. Electron Spectrosc. Relat. Phenom. **4**, 313 (1974).
[5] Y. Morioka, M. Nakamura, E. Ishiguro, and M. Sasanuma, J. Chem. Phys. **61**, 1462 (1974).
[6] R. B. Kay, Ph. E. van der Leeuw, and M. J. Van der Wiel, J. Phys. B **10**, 2513 (1977).
[7] D. M. Barrus, R. L. Blake, A. J. Burek, K. C. Chambers, and A. L. Pregenzer, Phys. Rev. A **20**, 1045 (1979).
[8] A. Bianconi, H. Petersen, F. C. Brown, and R. Z. Bachrach, Phys. Rev. A **17**, 1907 (1978).
[9] A. P. Hitchcock and C. E. Brion, J. Electron Spectrosc. Relat. Phenom. **18**, 1 (1980).
[10] M. Tronc, G. C. King, and F. H. Read, J. Phys. B **13**, 999 (1980).
[11] D. Dill, J. R. Swanson, S. Wallace, and J. L. Dehmer, Phys. Rev. Lett. **45**, 1393 (1980).
[12] C. M. Truesdale, S. H. Southworth, P. H. Kobrin, U. Becker, D. W. Lindle, H. G. Kerkhoff, and D. A. Shirley, Phys. Rev. Lett. **50**, 1265 (1983).
[13] D. W. Lindle, C. M. Truesdale, P. H. Kobrin, T. A. Ferrett, P. A. Heimann, U. Becker, H. G. Kerkhoff, and D. A. Shirley, J. Chem. Phys. **81**, 5375 (1984).
[14] U. Becker, R. Holzel, H. G. Kerkhoff, B. Langer, D. Szostak, and R. Wehlitz, Phys. Rev. Lett. **56**, 1445 (1986).
[15] A. Yagishita, H. Maezawa, M. Ukai, and E. Shigemasa, Phys. Rev. Lett. **62**, 36 (1989).
[16] E. Shigemasa, K. Ueda, Y. Sato, T. Hayaishi, H. Maezawa, T. Sasaki, and A. Yagishita, Phys. Scr. **41**, 63 (1990).
[17] N. Saito and H. Suzuki, Phys. Rev. Lett. **61**, 2740 (1988).
[18] K. Lee, D. Y. Kim, C. I. Ma, D. A. Lapiano-Smith, and D. M. Hanson, J. Chem. Phys. **93**, 7936 (1990).
[19] R. N. Zare, Mol. Photochem. **4**, 1 (1972).
[20] J. L. Dehmer and D. Dill, Phys. Rev. A **18**, 164 (1978).
[21] S. Wallace and D. Dill, Phys. Rev. B **17**, 1692 (1978).
[22] H. Maezawa, Y. Suzuki, H. Kitamura, and T. Sasaki, Appl. Opt. **25**, 3260 (1986).
[23] A. Yagishita, S. Masui, A. Toyoshima, H. Maezawa, and E. Shigemasa, Rev. Sci. Instrum. (to be published).
[24] A. Yagishita, Jpn. J. Appl. Phys. **25**, 657 (1986).
[25] T. Sasaki, in *Atomic Physics 10,* edited by H. Narumi and I. Shimamura (North-Holland, Amsterdam, 1987), p. 283.
[26] H. Kitamura (private communication).
[27] W. Eberhardt, J. Stöhr, J. Feldhaus, E. W. Plummer, and F. Sette, Phys. Rev. Lett. **51**, 2370 (1983).
[28] L. Ungier and T. D. Thomas, J. Chem. Phys. **82**, 3146 (1985).
[29] N. Saito and I. H. Suzuki, Chem. Phys. Lett. **129**, 419 (1986).
[30] G. R. Wight, M. J. Van der Wiel, and C. E. Brion, J. Phys. B **9**, 675 (1976).
[31] J. L. Dehmer and D. Dill, J. Chem. Phys. **65**, 5327 (1976).
[32] T. N. Rescigno and P. W. Langhoff, Chem. Phys. Lett. **51**, 65 (1977).
[33] A. V. Kondratenko, L. N. Mazalov, and K. M. Neiman, Zh. Strukt. Khim. **20**, 203 (1979).
[34] R. Arneberg, H. Ågren, J. Müller, and R. Manne, Chem. Phys. Lett. **91**, 362 (1982).
[35] A. Barth and J. Schirmer, J. Phys. B **18**, 867 (1985).
[36] C. T. Chen, Y. Ma, and F. Sette, Phys. Rev. A **40**, 6737 (1989).
[37] D. L. Lynch and V. McKoy, Phys. Rev. A **30**, 1561 (1984).